Local density of states in double-barrier resonant-tunneling structures

Thomas B. Bahder, John D. Bruno, Ralph G. Hay, and Clyde A. Morrison
U. S. Army Laboratory Command, Harry Diamond Laboratories, 2800 Powder Mill Road, Adelphi, Maryland 20783-1197
(Received 3 August 1987)

We calculate the local density of states between the barriers of a double-barrier resonant-tunneling structure within the context of a simplified model. As the area of the barriers increases, there is a smooth crossover in the density of states from a three-dimensional (3D) square-root-of-energy behavior to a 2D steplike behavior. The local 1D density of states corresponding to a fixed electron momentum transverse to the barriers is also calculated and shows sharp peaks at energies corresponding to the quasibound states between the wells. The width of the lowest quasibound state is computed as a function of barrier area.

I. INTRODUCTION

Recent advances in semiconductor growth techniques have led to a widespread interest in the physics of ultrasmall semiconducting systems. Quantum wells, superlattices, double-barrier resonant-tunneling structures, and a variety of other exotic structures have become the objects of extensive investigation.[1,2] The interest in these ultrasmall systems is motivated by two factors. First, their optical and electrical properties have quasi-two-dimensional (quasi-2D) features which frequently offer distinct advantages in device applications. Second, actual physical systems whose electron dynamics are quasi-2D provide one with a rich testing ground for theoretical models.

One of the systems attracting considerable attention is the double-barrier resonant-tunneling (DBRT) structure.[3] A typical structure consists of two thin ($\sim$50 Å) $Al_xGa_{1-x}As$ layers, separated by an equally thin ($\sim$50 Å) GaAs layer, all of which are embedded in a single GaAs crystal. The regions to the left and right of the barriers (usually beyond spacer layers) are n doped and are usually contacted for transport studies. Current-voltage characteristics of this device show an enhancement in the current when the applied voltage aligns the quasi-Fermi-energy of incoming electrons with the energies of the quasibound states in the quantum-well region. A number of theoretical calculations have been done to describe the nonlinear current response[4–16] in this system. However, controversy still exists regarding the basic mechanism behind the nonlinearity.[14,15,17–20] Despite the large number of studies to date, we have not found in the literature any calculation of the local density of states (DOS) for even a highly simplified model of a DBRT structure. The local DOS provides information about resonant states and gives one a measure of the extent to which the dynamics are quasi-2D. The purpose of this paper is to present such a calculation.

In Sec. II, using a simple model potential, we calculate the eigenvalues and eigenfunctions of an effective-mass Schrödinger equation. These results are used in Sec. III to compute the local DOS in the quantum-well region of the potential. In Sec. IV, we relate this local DOS to an integral of a one-dimensional (1D) DOS. This latter DOS has sharp peaks at energies corresponding to the quasibound states between barriers.

II. THE MODEL

We consider a simplified model, which is defined by the following effective-mass Hamiltonian:

$$H=-\frac{\hbar^2}{2m_c}\nabla^2+V(z)\ , \tag{1}$$

where m_c is the effective mass of electrons at the bottom of the GaAs conduction band and

$$V(z)=V_0\delta(z+a)+V_0\delta(z-a)\ . \tag{2}$$

In this model, the two $Al_xGa_{1-x}As$ potential barriers have been replaced by δ-function barriers of strength V_0, separated by a distance $2a$ along the z axis (the growth direction). The parameter V_0 is given by

$$V_0=b\Delta V_c\ , \tag{3}$$

where ΔV_c is the conduction-band discontinuity and b is the barrier width.

We solve the one-electron Schrödinger equation

$$H\Psi(\mathbf{r})=E\Psi(\mathbf{r}) \tag{4}$$

subject to periodic boundary conditions in the x and y directions

$$\Psi(x+L,y,z)=\Psi(x,y,z)\ , \tag{5a}$$

$$\Psi(x,y+L,z)=\Psi(x,y,z)\ . \tag{5b}$$

Since Eq. (4) is separable, we can write the wave function in the product form

$$\Psi(\mathbf{r})=\frac{1}{L}e^{i\mathbf{k}_\perp\cdot\mathbf{r}}\psi(z)\ , \tag{6}$$

where $k_\perp=(k_x,k_y,0)$, $k_x=2\pi n_x/L$, $k_y=2\pi n_y/L$, and n_x,n_y take the integer values $0,\pm1,\pm2,\ldots$. The z part of the wave function, $\psi(z)$, satisfies the reduced equation

$$\psi''(z)+\frac{2m_c}{\hbar^2}[\varepsilon-V(z)]\psi(z)=0 , \tag{7}$$

where $\varepsilon=E-\hbar^2\mathbf{k}_\perp^2/2m_c$. For $\psi(z)$, we choose the vanishing boundary conditions

$$\psi(-L/2)=0 , \tag{8a}$$

$$\psi(L/2)=0 . \tag{8b}$$

The presence of the δ functions imposes two jump-discontinuity conditions on the derivative of $\psi(z)$ at the δ-function positions, which are given by

$$\psi'(-a+0^+)-\psi'(-a-0^+)=\gamma\psi(-a) , \tag{9a}$$

$$\psi'(a+0^+)-\psi'(a-0^+)=\gamma\psi(a) , \tag{9b}$$

where $\gamma=2m_cV_0/\hbar^2$, and 0^+ is a positive infinitesimal quantity. These two conditions may be found by integrating Eq. (7) over the infinitesimal intervals $(-a-0^+,-a+0^+)$ and $(a-0^+,a+0^+)$. In addition, we require the wave function to be continuous at the δ-function positions

$$\psi(-a-0^+)=\psi(-a+0^+) , \tag{10a}$$

$$\psi(a-0^+)=\psi(a+0^+) . \tag{10b}$$

To look for a solution to Eq. (7), we take advantage of symmetry and solve the eigenvalue problem in the region $0<z<L/2$. We then look for even wave functions of the form

$$\psi_{ek}(z)=\begin{cases} A_1(k)\cos(kz), & 0<z<a \\ A_2(k)\cos(kz)+A_3(k)\sin(kz), & a<z<\dfrac{L}{2} \end{cases} \tag{11}$$

and odd wave functions of the form

$$\psi_{ok}(z)=\begin{cases} B_1(k)\sin(kz), & 0<z<a \\ B_2(k)\cos(kz)+B_3(k)\sin(kz), & a<z<\dfrac{L}{2} \end{cases} . \tag{12}$$

For the even wave functions, when we impose the conditions in Eqs. (8b), (9b), and (10b), we get a set of three homogeneous equations for $A_1(k)$, $A_2(k)$, and $A_3(k)$. To have a nontrivial solution, we require the determinant of the coefficient matrix to vanish. This gives an equation for the allowed k's which label the even parity states:

$$\frac{\gamma}{k}\cos(ka)\sin(kl-ka)+\cos(kl)=0 . \tag{13a}$$

Here we have used the convenient definition $l=L/2$. Solving the three homogeneous equations for the ratios, we find

$$\frac{A_3(k)}{A_1(k)}=\frac{\gamma}{k}\cos^2(ka) , \tag{13b}$$

$$\frac{A_2(k)}{A_1(k)}=1-\frac{\gamma}{k}\sin(ka)\cos(ka) . \tag{13c}$$

Applying the same boundary conditions to the odd solutions given in Eq. (12) and setting the determinant of the coefficient matrix to zero leads to the equation satisfied by the allowed wave vectors labeling the odd-parity states:

$$\frac{\gamma}{k}\sin(ka)\sin(kl-ka)+\sin(kl)=0 . \tag{14a}$$

Solving the associated system of equations leads to

$$\frac{B_2(k)}{B_1(k)}=-\frac{\gamma}{k}\sin^2(ka) , \tag{14b}$$

$$\frac{B_3(k)}{B_1(k)}=1+\frac{\gamma}{k}\sin(ka)\cos(ka) . \tag{14c}$$

The constants A_1 and B_1 are evaluated from the normalization condition

$$\int_{-l}^{+l}|\psi_{\alpha k}(z)|^2dz=1 ,$$

where $\alpha=e$ (o) for the even (odd) solutions. We find

$$\frac{1}{A_1^2(k)}=l\left\{1+\frac{\sin(2ka)}{2kl}+\left[1-\frac{a}{l}\right]\left[\left[\frac{\gamma}{2k}\right]^2\sin^2(2ka)-\frac{\gamma}{k}\sin(2ka)+\left[\frac{\gamma}{k}\right]^2\cos^4(ka)\right]\right.$$
$$+\frac{1}{kl}\cos[k(l+a)]\sin[k(l-a)]\left[\left[\frac{\gamma}{2k}\right]^2\sin^2(2ka)-\frac{\gamma}{k}\sin(2ka)-\left[\frac{\gamma}{k}\right]^2\cos^4(ka)+1\right]$$
$$\left.-\frac{2}{kl}\frac{\gamma}{k}\left[\frac{\gamma}{2k}\sin(2ka)-1\right]\cos^2(ka)\sin[k(l+a)]\sin[k(l-a)]\right\} , \tag{15}$$

and

$$\frac{1}{B_1^2(k)}=l\left\{1-\frac{\sin(2ka)}{2kl}+\left[1-\frac{a}{l}\right]\frac{\gamma}{k}\left[\sin(2ka)+\frac{\gamma}{k}[\sin^4(ka)+\tfrac{1}{4}\sin^2(2ka)]\right]\right.$$

$$+\frac{1}{kl}\cos[k(l+a)]\sin[k(l-a)]\left[\left[\frac{\gamma}{k}\right]^2[\sin^4(ka)-\tfrac{1}{4}\sin^2(2ka)]-\frac{\gamma}{k}\sin(2ka)-1\right]$$

$$-\frac{2}{kl}\frac{\gamma}{k}\left[\frac{\gamma}{2k}\sin(2ka)+1\right]\sin^2(ka)\sin[k(l+a)]\sin[k(l-a)]\Bigg\} . \tag{16}$$

The energy eigenvalues associated with the eigenfunctions in Eqs. (11) and (12) are given by

$$E_{\mathbf{k}\alpha}=\frac{\hbar^2\mathbf{k}^2}{2m_c} . \tag{17}$$

With vanishing boundary conditions on $\psi(z)$ at $z=\pm l$, the limit of zero-strength δ functions ($\gamma\to 0$) is identical to the limit where the δ functions are placed on the boundaries ($a\to l$). In both cases one recovers the 1D particle-in-a-box problem, where $A_3/A_1=B_2/B_1=0$, $A_2/A_1=B_3/B_1=1$, and $A_1=B_1=(2/L)^{1/2}$.

III. 3D DENSITY OF STATES

We now construct the single-particle Green's function

$$G(\mathbf{r},\mathbf{r}';E)=\sum_{\mathbf{k}_\perp}\sum_{\alpha}\sum_{k_\alpha}\frac{\Psi_{\alpha\mathbf{k}}(\mathbf{r})\Psi^*_{\alpha\mathbf{k}}(\mathbf{r}')}{E-E_{\mathbf{k}}+i0^+} , \tag{18}$$

where the eigenstates $\Psi_{\alpha\mathbf{k}}(\mathbf{r})$ are given by Eqs. (6), (11), and (12), and $\mathbf{k}=(\mathbf{k}_\perp,k_\alpha)$. Here α ($=e$ or o) labels a state's parity, $\mathbf{k}_\perp=(k_x,k_y)$, and k_α are given by the roots of Eqs. (13a) and (14a) for even- and odd-parity states, respectively. Using the Green's function, we calculate the local DOS (including both spins):

$$D(z,E)=-\frac{2}{\pi}\mathrm{Im}G(\mathbf{r},\mathbf{r};E) \tag{19}$$

$$=\frac{2}{L^2}\sum_{\mathbf{k}_\perp}\sum_{\alpha}\sum_{k_\alpha}|\psi_{\alpha k_\alpha}(z)|^2\delta(E-E_{\mathbf{k}}) . \tag{20}$$

In the limit when the system size goes to infinity, with a held constant, the density of allowed wave vectors becomes $2\pi/L$. This allows us to change the sums in Eq. (20) to integrals

$$D(z,E)=\frac{L}{4\pi^3}\int_{-\infty}^{+\infty}d^2k_\perp \times\int_0^\infty dk\sum_{\alpha}|\psi_{\alpha k}(z)|^2\delta(E-E_{\mathbf{k}}) . \tag{21}$$

The integration over $\mathbf{k}_\perp=(k_x,k_y)$ is over all positive and negative wave vectors, whereas the z-component wave vector k is integrated over positive values only. Using the explicit form of the wave functions and changing to spherical momentum coordinates, we have for the region $-a<z<+a$

$$D(z,E)=\frac{1}{8a_0^3E_0}\int_0^{(\pi/2)(E/E_0)^{1/2}}dq\left[F_e(q)\cos^2\left[\frac{z}{a}q\right]+F_o(q)\sin^2\left[\frac{z}{a}q\right]\right], \tag{22}$$

where

$$F_e(q)=\frac{q^2}{q^2+U^2\cos^2(q)-Uq\sin(2q)}=\frac{1}{\left|1+\frac{iU}{2q}(1+e^{i2q})\right|^2} , \tag{23a}$$

$$F_o(q)=\frac{q^2}{q^2+U^2\sin^2(q)+Uq\sin(2q)}=\frac{1}{\left|1+\frac{iU}{2q}(1-e^{i2q})\right|^2} , \tag{23b}$$

the dimensionless potential strength U is defined by $U=\gamma a=2mV_0a/\hbar^2$, and a convenient energy scale, $E_0=\pi^2\hbar^2/8m_ca^2$, has been introduced. The functions $F_e(q)$ and $F_o(q)$ are related to the wave-function amplitudes by

$$\lim_{a/l\to 0} lA_1^2\left[\frac{q}{a}\right]=F_e(q) ,$$

$$\lim_{a/l\to 0} lB_1^2\left[\frac{q}{a}\right]=F_o(q) .$$

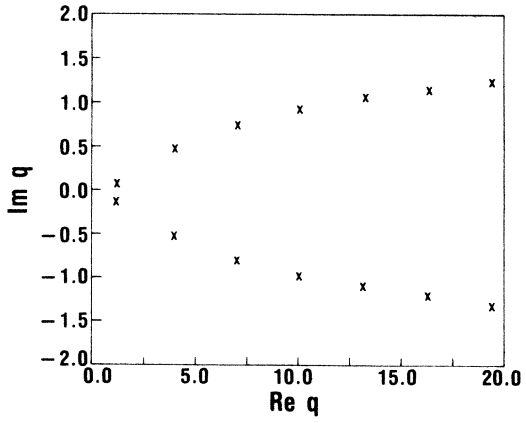

FIG. 1. The locations of the poles of $F_e(q)$ are shown for $U=3$. The poles of $F_o(q)$ (not shown) lie between the poles of $F_e(q)$.

The local DOS of states given by Eq. (22) is a sum of two terms. The term containing $F_e(q)$ gives the local density of even states in the well, and the term with $F_o(q)$ gives the local density of odd states. Each function $F_\alpha(q)$, $\alpha = e$ or o, is an even function with an infinite sequence of (complex-conjugate) pairs of simple poles in the complex q plane (see Fig. 1). Each pair of poles with $\mathrm{Re}(q) > 0$ corresponds to one resonance. In the limit $U \to 0$ (no δ-function barriers), these poles move away from the real-q axis to infinity and $F_\alpha(q) \to 1$ on the real axis. In this limit, $D(z,E)$ is simply the local DOS for a free-electron gas in a box of volume $2aL^2$.

As we approach the limit of strong barriers, $U \gg 1$, the poles of the functions $F_\alpha(q)$ move in toward the real axis in pairs (one pole above and one pole below) (see Fig. 1). In the region of $U \gg 1$, and $0 < q \lesssim U$, the functions $F_\alpha(q)$ are well represented by a sum of Lorentzians

$$F_\alpha(q) \sim \sum_n \frac{\Gamma_{\alpha n}}{(q - q_{\alpha n})^2 + \Gamma_{\alpha n}^2} , \tag{24}$$

where the real and imaginary positions of the poles, $q_{\alpha n} \pm i\Gamma_{\alpha n}$, are functions of U. For $U \to \infty$, we have $\Gamma_{\alpha n} \to 0$, $q_{en} \to (2n+1)\pi/2$, and $q_{on} \to n\pi$.

In this limit we find

$$\lim_{U \to \infty} F_\alpha(q) \to \pi \sum_n \delta(q - q_{\alpha n}) . \tag{25}$$

Rather than look at the local DOS in more detail, we consider its integral over the well volume

$$N(E) = \frac{mL^2}{\pi^2\hbar^2} \int_0^{(\pi/2)(E/E_0)^{1/2}} dq \left[F_e(q) + F_o(q) + [F_e(q) - F_o(q)] \times \frac{\sin(2q)}{2q} \right] . \tag{26}$$

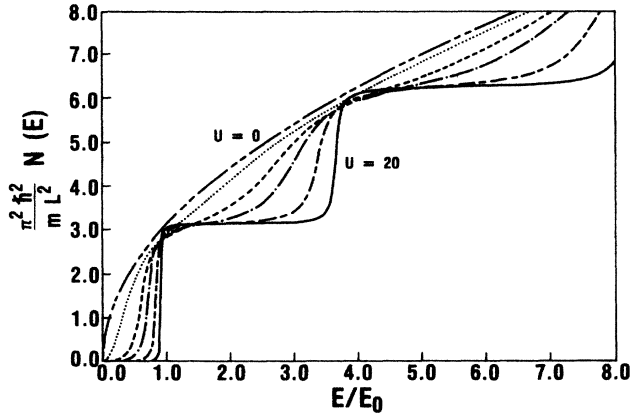

FIG. 2. The dimensionless DOS between barriers, $(\pi^2\hbar^2/mL^2)N(E)$, is plotted as a function of dimensionless electron energy, E/E_0, for values of $U = 0, 1, 3, 5, 10, 20$. Higher values of U correspond to an increased steplike structure.

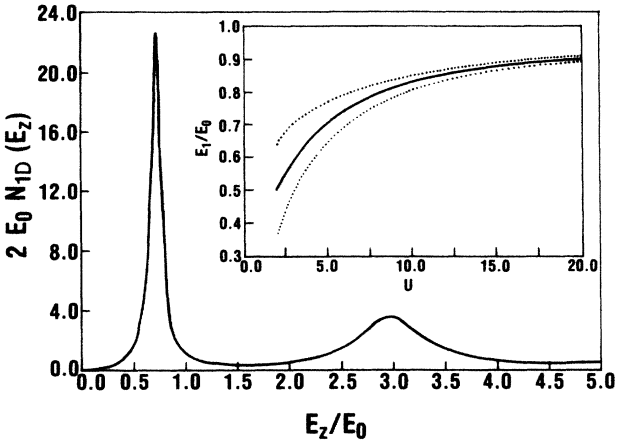

FIG. 3. On the outer axis, a plot of $2E_0N_{1D}(E_z)$ vs E_z/E_0 is shown. In the inset, the solid line is a plot of the energy of the lowest resonance (lowest energy peak in the DOS) vs the dimensionless potential U. The vertical distance between the dotted curves gives the full width at half maximum of the lowest resonant level, as a function of U.

The function $N(E)$ gives the number of states in the well per unit energy interval. In the limit of weak barriers, $U \ll 1$, we find

$$N(E) \xrightarrow{U \to 0} \frac{1}{2\pi^2} \left(\frac{2m}{\hbar^2} \right)^{3/2} 2aL^2\sqrt{E} ,$$

which is the DOS for a free-electron gas in a volume $2aL^2$.

In the limit of strong barriers, $U \gg 1$, we find

$$N(E) \xrightarrow{U \to \infty} \frac{mL^2}{\pi\hbar^2} \sum_{n=1}^{\infty} \Theta(E - n^2E_0) , \tag{27}$$

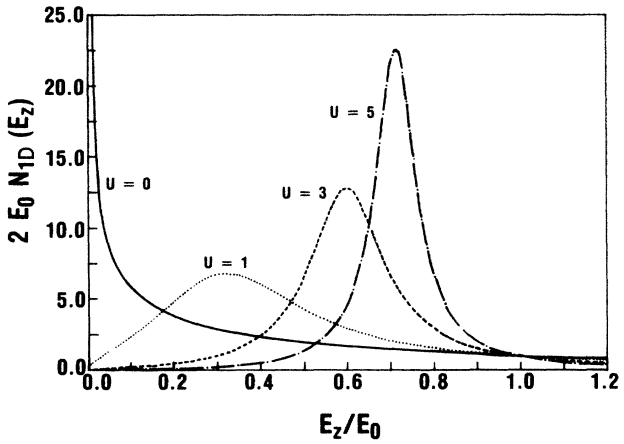

FIG. 4. The 1D DOS, $2E_0N_{1D}(E_z)$, is plotted vs E_z/E_0 in the region of the resonance peak for several values of U.

where $\Theta(x)=1$ for $x>0$ and $\Theta(x)=0$ for $x<0$. This is the well-known staircaselike DOS one would expect in a quasi-2D system. For intermediate values of U, the DOS $N(E)$ is plotted in Fig. 2.

IV. 1D DENSITY OF STATES

Since the Hamiltonian in Eq. (1) conserves transverse electron momentum, k_x and k_y are good quantum numbers, and an electron placed in a state of definite $\mathbf{k}_\perp$ will remain in this state indefinitely. With this in mind we consider the Green's function

$$G_{1D}(\mathbf{r},\mathbf{r}';E)=\sum_{\alpha}\sum_{k_\alpha}\frac{\Psi_{\alpha\mathbf{k}}(\mathbf{r})\Psi^{*}_{\alpha\mathbf{k}}(\mathbf{r}')}{E-E_{\mathbf{k}}+i0^{+}}\ , \tag{28}$$

in which the summation on $\mathbf{k}_\perp$ is omitted. Using this Green's function we define the 1D local DOS (including both spins) by

$$\begin{aligned}D_{1D}(z,E_z)&=-\frac{2}{\pi}\mathrm{Im}G_{1D}(\mathbf{r},\mathbf{r};E)\\&=\frac{1}{L^2}\sum_{\alpha}\sum_{k_\alpha}|\psi_{\alpha k_\alpha}(z)|^2\\&\quad\times\delta\left[E-\frac{\hbar^2\mathbf{k}_\perp^2}{2m_c}-\frac{\hbar^2k_\alpha^2}{2m_c}\right],\end{aligned} \tag{29}$$

where $\psi_{\alpha k_\alpha}(z)$ is given in Eqs. (11) and (12), and $E_z=E-\hbar^2\mathbf{k}_\perp^2/2m_c$. The function $D_{1D}(z,E_z)$ gives the number of states (labeled by α and k_α) per unit volume, for a given $\mathbf{k}_\perp$. This function displays peaks which are associated with the resonances. Substituting the explicit form of the wave functions into Eq. (29), we find

$$\begin{aligned}D_{1D}(z,E_z)=\frac{1}{2aL^2E_0\sqrt{\varepsilon}}&\left[F_e\left[\frac{\pi}{2}\sqrt{\varepsilon}\right]\cos^2\left[\frac{\pi z}{2a}\sqrt{\varepsilon}\right]\right.\\&\left.+F_o\left[\frac{\pi}{2}\sqrt{\varepsilon}\right]\sin^2\left[\frac{\pi z}{2a}\sqrt{\varepsilon}\right]\right],\end{aligned} \tag{30}$$

where the dimensionless z component of energy, ε, is defined by $\varepsilon=E_z/E_0$. Again, rather than looking at this in more detail, we consider the integral of $D_{1D}(z,E_z)$ over the well volume

$$\begin{aligned}N_{1D}(E_z)&=\int_{\text{well}}D_{1D}(z,E_z)d^3r\\&=\frac{1}{2E_0\sqrt{\varepsilon}}\left[F_e\left[\frac{\pi}{2}\sqrt{\varepsilon}\right]\left[1+\frac{\sin(\pi\sqrt{\varepsilon})}{\pi\sqrt{\varepsilon}}\right]\right.\\&\quad\left.+F_o\left[\frac{\pi}{2}\sqrt{\varepsilon}\right]\left[1-\frac{\sin(\pi\sqrt{\varepsilon})}{\pi\sqrt{\varepsilon}}\right]\right].\end{aligned} \tag{31}$$

This function specifies the number of states in the well labeled by α,k_α, per unit energy, for a given $\mathbf{k}_\perp$. In the limit of weak barriers, $U\to 0$, the function $N_{1D}(E_z)\to 1/(E_0\varepsilon^{1/2})$ which is the DOS for a 1D free-electron gas. In the limit of strong barriers, $U\to\infty$, the number of states in the well per unit energy is just a sum of δ functions. In this limit the resonant states are the eigenstates of the 1D particle-in-a-box problem and the resonance peaks shift to the appropriate limiting eigenvalues. For intermediate values of U (and energies $0<\varepsilon\lesssim U$), the function $N_{1D}(E_z)$ is approximately a sum of Lorentzians (see Fig. 3). The lowest energy peak is composed predominantly of even wave functions, while the second peak is composed mostly of the odd wave functions. In Fig. 4 we show the DOS $N_{1D}(E)$ for several values of U, in the energy region of the lowest resonant level. The inset of Fig. 3 shows the peak position of the lowest resonance as a function of barrier strength U. For energies much larger than U, $\varepsilon\gg U$, the functions $F_\alpha((\pi/2)\sqrt{\varepsilon})\to 1$ and the DOS returns to its value in the absence of barriers, $N_{1D}(E_z)\to 1/(E_0\sqrt{\varepsilon})$.

V. SUMMARY

Within the context of a simple model for a double-barrier structure, we solved for the normalized eigenstates. Using these eigenstates we calculated the 3D local DOS between the barriers. This quantity shows a crossover from a 3D square-root-of-energy behavior to a quasi-2D staircaselike behavior, as the barrier strength U is increased. For electron energies $\varepsilon\gg U$ the DOS always returns to the free-electron DOS. We also calculated the 1D DOS for a given transverse momentum $\mathbf{k}_\perp$. This quantity shows sharp peaks at energies corresponding to the resonant states. In a more realistic model, one can use the width of the lowest peak in $N_{1D}(E_z)$ to reliably estimate the lifetime of the lowest quasibound state. The inverse of this lifetime gives an estimate of the characteristic frequency above which resonant contribution to the current becomes negligible.

[1] See, for instance, *Synthetic Modulated Structures*, edited by L. L. Chang and B. C. Giessen (Academic, New York, 1985).

[2] For a more recent review see IEEE J. Quantum Electron. **QE-22**, 9 (1986).

[3] For an excellent discussion of the physics of resonant tunneling, see B. Ricco and M. Ya. Azbel, Phys. Rev. B **29**, 1970 (1984).

[4] J. C. Penley, Phys. Rev. **128**, 596 (1962).

[5] R. Tsu and L. Esaki, Appl. Phys. Lett. **22**, 562 (1973).

[6] M. C. Payne, J. Phys. C **19**, 1145 (1986).

[7] J. R. Barker, Physica **134B**, 22 (1985).

[8] U. Ravaioli, M. A. Osman, W. Potz, N. Kluksdahl, and D. K. Ferry, Physica **134B**, 36 (1985).

[9] H. Ohnishi, T. Inata, S. Muto, N. Yokoyama, and A. Shibatomi, Appl. Phys. Lett. **49**, 1248 (1986).

[10] P. J. Price, Superlatt. Microstruct. **2**, 213 (1986); **2**, 593 (1986).

[11] W. R. Frensley, J. Vac. Sci. Technol. **3**, 1261 (1985).

[12] W. R. Frensley, Phys. Rev. Lett. **57**, 2853 (1986).

[13] A. C. Marsh, IEEE J. Quantum Electron. **QE-23**, 371 (1987).

[14] S. Luryi, Appl. Phys. Lett. **47**, 490 (1985).

[15]T. Weil and B. Vinter, Appl. Phys. Lett. **50**, 1281 (1987).
[16]V. J. Goldman, D. C. Tsui, J. E. Cunningham, and W. T.Tsang, J. Appl. Phys. **61**, 2693 (1987).
[17]V. J. Goldman, D. C. Tsui, and J. E. Cunningham, Phys. Rev. Lett. **58**, 1256 (1987).
[18]H. Morkoc, J. Chen, U. K. Reddy, T. Henderson, and S. Luryi, Appl. Phys. Lett. **49**, 70 (1986).
[19]E. Wolak, A. Harwit, and J. S. Harris, Jr., Appl. Phys. Lett. **50**, 1610 (1987).
[20]T. B. Bahder, C. A. Morrison, and J. D. Bruno, Appl. Phys. Lett. **51**, 1089 (1987).